

**2012 NDIA GROUND VEHICLE SYSTEMS ENGINEERING AND TECHNOLOGY  
SYMPOSIUM  
POWER AND MOBILITY (P&M) MINI-SYMPOSIUM  
AUGUST 14-16, MICHIGAN**

**AN EXPERIMENTAL INVESTIGATION TO IMPROVE LEAD ACID  
BATTERY RECHARGING ALGORITHMS FOR ENVIRONMENTAL  
PERFORMANCE**

**Stanley Jones, PhD**

**John Mendoza, PhD**

**Daniel Wang**

Science Applications International Corporation

**Yi Ding, PhD**

**Sonya Zanardelli**

Tank-Automotive Research, Development Engineering Center

**ABSTRACT**

*An experimental testing program has been developed that looks to optimize the battery recharging algorithms to improve battery lifetime and state of charge knowledge. The first phase of the testing targeted lead acid battery performance characterization as a function of controlled environmental temperatures. Subsequent testing includes performance testing under alternator recharging using default and proposed charging algorithms. A new experimental apparatus has been developed to integrate battery testing with alternator charging to simulate in-vehicle operations under controlled environmental conditions. Results are presented for the baseline performance testing, a model is presented for the characterization of battery parameters and a description of the test apparatus and approach employed for the integrated alternator testing is included.*

**INTRODUCTION**

Lead acid batteries function as the principle energy storage media for most military ground vehicles. These batteries provide power for starting, lighting, and ignition (SLI) functions. The vehicle alternator or generator systems then provide battery recharge functionality. These power demands typically represent a shallow battery discharge. However, the demand for power during silent watch operations presents an increasing demand on battery function, thereby, imposing a greater demand on battery depth of discharge. Accurate knowledge of battery reserve capacity can be crucial to mission performance. Furthermore, in application, lead acid batteries are subject to a wide range of environmental conditions that can detrimentally affect battery lifetime. Replacement batteries represent a significant cost and logistics burden to ground vehicle fleet operations.

Vehicle alternator systems typically provide a constant voltage power – adjusted to ambient temperature – to recharge the vehicle batteries. However, temperature compensation is often adjusted as a function of local

alternator temperature rather than the temperature of the battery. Vehicle packaging considerations may imply that the vehicle battery and the alternator are not collocated and, therefore, may not share identical environmental conditions. Furthermore, the constant voltage algorithms used to provide alternator power may not represent the most ideal recharging functionality.

**PROGRAM OVERVIEW**

A series of tests have been developed and are under execution to characterize battery performance as a function of battery state-of-charge and temperature. The first phase of testing has provided the fundamental data to establish the parameters of an effective battery equivalent circuit model. Subsequent testing will look to characterize and optimize the effectiveness of proposed charging protocols.

Experimental sequences are controlled with an Advanced Battery Tester Unit to perform charge and discharge capacity measurements in accordance with standard military battery specifications. Data collected included current, voltage, and cell surface temperatures over the course of each experiment. These data allowed for calculations of the

battery open circuit voltage and effective series resistance as a function of battery state-of-charge.

A vehicle simulation apparatus incorporating a military alternator has been developed. Testing with this apparatus will characterize and compare charging algorithm performance during realistic silent watch, vehicle ignition and driving sequences.

### ALTERNATOR FUNCTIONALITY

Vehicle alternators typically employ a controlled output at a constant voltage to achieve battery recharging as well as meeting system load demands. This is generally accomplished through adjustment of the rotor – stator magnetic coupling by adjustment of the rotor coil current. Output voltage is maintained constant, as measured at the alternator output or battery terminals to provide battery re-charging current and vehicle power demands. A typical representation of an alternator wiring schematic is shown in Figure 1.

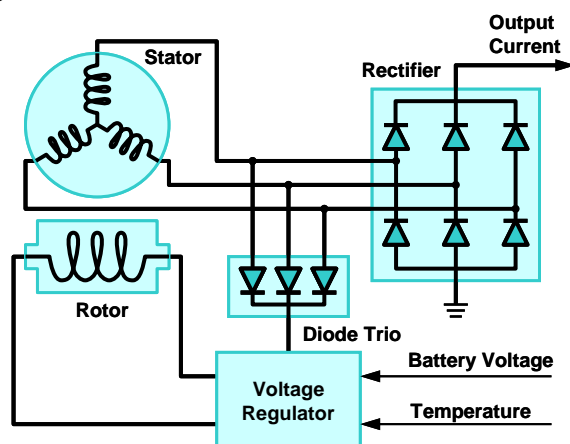


Figure 1: Typical Alternator Layout

To compensate for the temperature effects on battery functionality, high performance alternators often employ a temperature compensation scheme to account for reduced charge acceptance at elevated temperatures. The temperature compensation scheme for a commercially available military quality alternator [1] is shown in Figure 2.

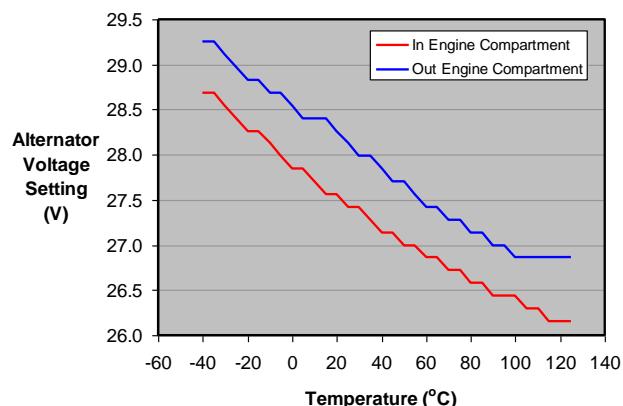


Figure 2: Alternator Voltage Setting Temperature Response

The use of temperature compensation schemes, such as those shown in Figure 2, improve battery lifetime by reducing the detrimental effects of overcharging at elevated temperatures. Temperature feedback may be used to enhance the fidelity of battery voltage control. This approach requires local instrumentation to ensure that the alternator output responds to battery temperature. This is particularly true when the battery and alternator are not collocated in the vehicle.

Since the alternator controls the output voltage, charging current is supplied to the battery in accordance with the effective resistance of the battery itself. Temperature-based compensation looks to account for the changes in battery resistance to limit charging current to reasonable values.

Although measures are taken to compensate for temperature effects, standard alternator circuits provide no means for active compensation to account for battery state-of-charge (SOC) effects. It is well known that battery voltage decays as a function of SOC. Charging current to the battery is driven by the difference between the battery voltage and the alternator output. However, the effective battery resistance also changes as a function of the battery SOC.

In automotive applications, the depth of discharge for a battery is typically small. However, with the advent of silent watch operations, the desire to utilize greater depth of discharge is evident. As a greater range of the battery

capacity is utilized, compensation of SOC effects to the charging protocols has increasing import.

It has been proposed that an improved alternator charging algorithm can be developed compensating for both temperature and SOC effects that will optimize charging functionality to improve battery lifetime. To meet this end, a series of environmental tests have been conducted to characterize battery performance and provide input for development of a functional model for battery performance.

### MODEL DEVELOPMENT

Many forms of equivalent circuit models have been developed for characterization of lead acid battery performance, ranging from resistor-capacitor (R-C) forms to overall impedance models [2]-[5]. The most common form utilized is the Thevinin model depicted in Figure 3. This model utilizes an open circuit voltage (OCV) source coupled to an R-C element in series with an output resistor. The R-C element provides for battery cell voltage relaxation. The parallel leg accounts for parasitic drain during charging operations.

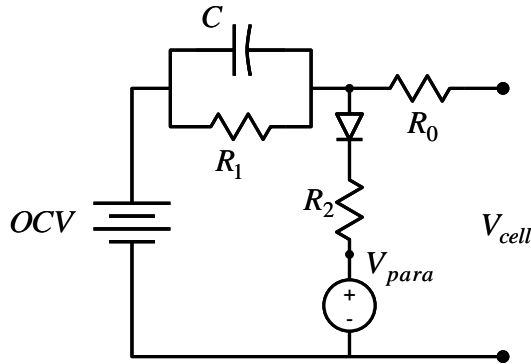


**Figure 3:** Thevinin Equivalent Circuit Model

The line resistances ( $R_1$  and  $R_0$ ) are actually unique functions of whether the battery is undergoing charge or discharge. Under discharging, the line resistance (or direct current resistance) is typically significantly lower than during charging operations. It is therefore desirable to characterize these resistances independently.

It is desirable to have the equivalent circuit model respond dynamically to battery status and operating conditions. To this end, the open circuit voltage (OCV) can be characterized as a function of battery state of charge while the resistance values and capacitance are assumed to be functions of both temperature and SOC.

$$OCV = f(SOC)$$

The state of charge of the cell is determined by integrating the current demand over time through the expression:

$$SOC = SOC_{t=0} - \frac{1}{C(\bar{I}, \theta)} \int_0^t I(\tau) d\tau$$

where  $C$  represents the capacity of the cell as a function of the local time averaged current,  $\bar{I}$ , and the dimensionless cell temperature,  $\theta$ .

A general form for correlation of the cell open circuit voltage can be written as:

$$OCV = Ae^{-\alpha x} + B[1 - e^{-\beta(1-x)}] + Cx + D$$

where the coefficients ( $A$ ,  $B$ ,  $C$ ,  $D$ ,  $\alpha$ , and  $\beta$ ) are tuned to the performance of the cell and  $x$  represents the fractional depth of discharge. This functional form has a great deal of flexibility to handle the non-linear behavior at near-full and near-empty battery conditions.

For the lead acid battery under consideration in this study (a commercial available valve regulated 6TAGM) the open circuit voltage data points and correlation curve fit are shown in Figure 4.

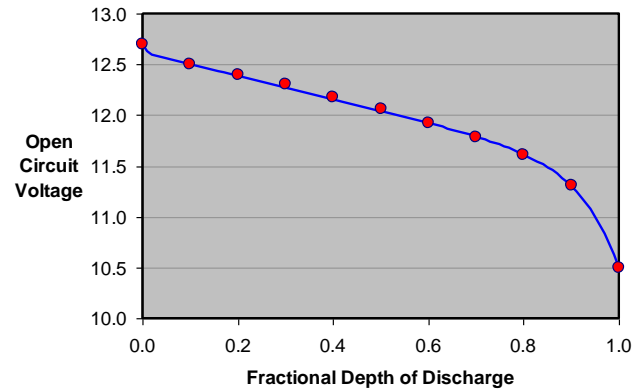


**Figure 4:** Open Circuit Voltage as a function of Battery Depth of Discharge

A least squared error approach allowed for determination of the OCV coefficients listed in Table 1.

**Table 1:** OCV Correlation Coefficients

Coefficient	Value
$A$	0.086
$B$	0.969
$\alpha$	115.664
$\beta$	12.203
$C$	-1.145
$D$	11.645

It is well known that the cell capacity is a function of the current rate drawn from the cell. Functionally, determination of the cell capacity in the state-of-charge calculation can take many forms. Classically, the cell capacity can be determined Peukert's Law:

$$C(I) = (I_0/I)^{k-1} C_0$$

where  $I_0$  and  $C_0$  represent the nameplate performance of the cell and  $k$  is a coefficient unique to each battery type. Peukert's Law suffers from several shortcomings. It tends to overestimate the capacity at high current values and there is no provision for temperature compensation.

A more general correlation for capacity formulation as a function of current demand has been used [6] of the form:

$$C(I) = \frac{\alpha}{1 + (\alpha - 1)(I/I_0)^\beta} C_0$$

However, through tuning of the manufacturer data, a higher fidelity model form has been found of the form:

$$C(I) = \frac{\alpha(I/I_0)^\gamma}{1 + (\alpha - 1)(I/I_0)^\beta} C_0$$

where  $\alpha$ ,  $\beta$ ,  $\gamma$  represent correlation coefficients unique to each battery type. A comparison of the best-fit capacity correlations for each of the three models to the manufacturer data are shown in Figure 5. The modified correlation captures both low and high current operations better than the general correlation. Best-fit coefficients for the general and modified correlations are listed in Table 2.

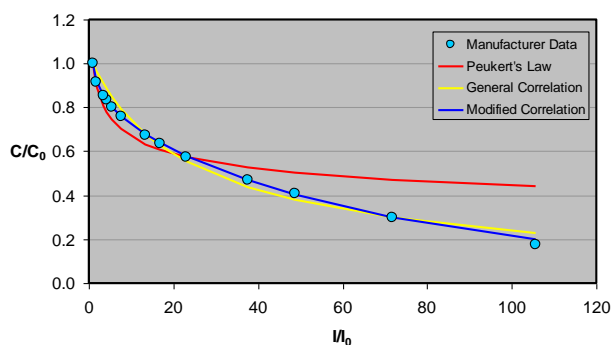


**Figure 5:** Comparison between Cell Capacity Correlations and Manufacturer Data for the valve regulated 6TAGM Battery

**Table 2:** Cell Capacity Correlation Coefficients

	General Correlation	Modified Correlation
$\alpha$	1.073	1.001
$\beta$	0.808	1.532
$\gamma$	N/A	-0.122

## ENVIRONMENTAL TESTING

Environmental testing to characterize the capacity effects associated with temperature was conducted according to the military standard reserve capacity test [7] using the SAIC-developed Advanced Battery Tester coupled to an environmental chamber. In these tests discharge sequences were conducted at a constant current of 25 A to a cut-off voltage of 10.5 V. Charging sequences were conducted with a constant voltage of 14.25 V for 10 hours. An exemplar set of test data is shown in Figure 6.

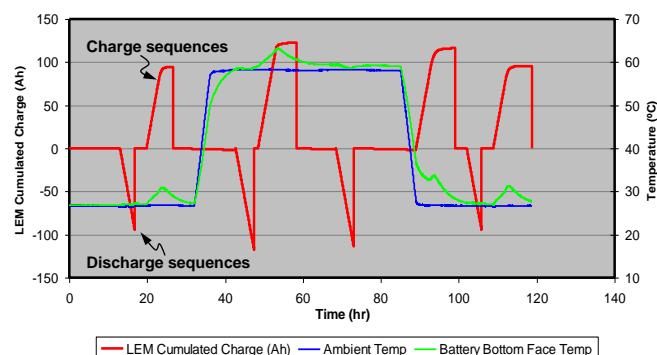


**Figure 6:** Exemplar Environmental Performance Testing

In the environmental performance testing batteries were first tempered to 27°C in an environmental chamber. A pre-test baseline performance was captured with a discharge and charge sequence at that temperature. The environmental chamber temperature was then ramped up to the desired target temperature and the cell temperature was allowed to reach steady-state conditions. A discharge and recharge sequence was then executed followed by a subsequent discharge at the target temperature. The test article temperature was then raised back to 27°C and a charge, discharge and recharge sequence executed. Tests were performed at controlled target temperatures of -30, -15, 0, 15, 45 and 60°C. Cell current, voltage and temperature response were recorded throughout.

### Capacity Temperature Correction

The battery capacities determined from the reserve capacity tests were calculated and compared to the capacity measured at the nominal temperature (27°C). These data points are depicted in Figure 7.

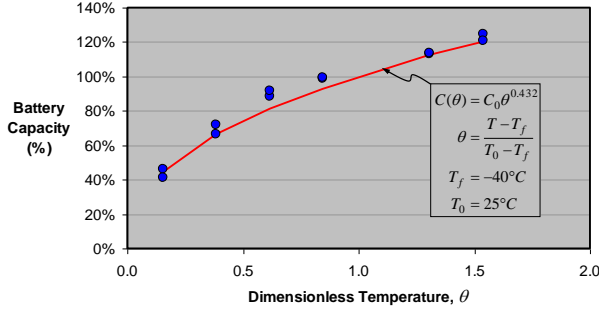


**Figure 7:** Percent Capacity as a Function of Cell Temperature

A product formulation is desired for the temperature capacity correction such that it can be simply integrated with the current correction factor. To meet that end, a simple power law format was chosen of the form:

$$C(\theta) = C_0 \theta^\delta$$

where  $\delta$  is a correlation coefficient and  $\theta$  represents a dimensionless temperature defined by:

$$\theta = \frac{T - T_f}{T_0 - T_f}$$

In this characterization, the temperature limits ( $T_0$  and  $T_f$ ) are somewhat arbitrary. However,  $T_0$  should be chosen to provide a value of unity at the nameplate capacity,  $C_0$ . For this case,  $T_f$  was selected at the approximate electrolyte freezing temperature of  $-40^\circ\text{C}$ .

$$T_f = -40^\circ\text{C}$$

$$T_0 = 25^\circ\text{C}$$

Coupling the temperature correction factor with the current correlation provides a suggested functional form for battery capacity correction:

$$C(I, \theta) = \frac{\alpha(I/I_0)^\gamma \theta^\delta}{1 + (\alpha - 1)(I/I_0)^\beta} C_0$$

This correlation provides for capacity correction from battery nameplate values for current and temperature in terms of four coefficients ( $\alpha$ ,  $\beta$ ,  $\gamma$ , and  $\delta$ ) unique to a particular battery type.

### Cell Resistance

Another key result from environmental testing is the ability to capture the equivalent resistance of the battery cell as a function of temperature and state-of-charge. The battery direct current resistance (DCR) can be determined from the following function:

$$DCR = \left| \frac{\text{Cell Voltage} - \text{OCV}}{\text{Cell Current}} \right|$$

Subtracting the cell OCV from the real time measured cell voltage provides a measure of the sum of the line resistances in the equivalent circuit model. Note that since the battery currents are maintained constant, the capacitor in the equivalent circuit only participates in the short term at the very beginning of a sequence and recovery after a test is completed. However, even with this simplification, the calculated DCR values are highly non-linear.

Because the battery SOC ranges from values of zero to unity, a convenient format for correlation is two exponential functions superimposed with a linear function similar to the OCV correlation:

$$DCR = Ae^{-\alpha \text{SOC}} + Be^{-\beta(1-\text{SOC})} + C\text{SOC} + D$$

This correlation has six coefficients that can be tuned to provide resistance estimates as a function of cell SOC. To extend this correlation further, a linear temperature fit of each of these coefficients have been developed of the form:

$$\text{Coefficients, } (A, B, \alpha, \beta, C, D) = m\theta + b$$

For battery charging, the resultant DCR data and correlation curve fits are depicted in Figure 8. The correlation provides astounding good correlation to the measured data.

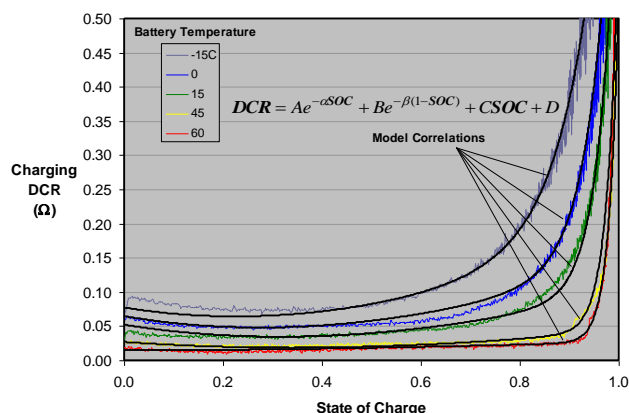


**Figure 8:** Charging DCR Data and Model Correlation as a function of Battery SOC and Temperature

Coefficient data obtained from least squared error minimization for the charging resistance model are shown in Table 3.

**Table 3:** Charging Resistance Model Temperature Coefficients

Coefficient	m	B
<i>A</i>	-1.113	1.753
<i>B</i>	-0.308	0.980
<i>α</i>	0.129	0.602
<i>β</i>	33.369	0.797
<i>C</i>	-0.616	0.982
<i>D</i>	1.059	-1.655

To improve the charging characteristics of the battery, the charging resistance and knowledge of the battery SOC are needed.

Discharging resistance is generally significantly lower than charging resistance and does not exhibit the same extreme growth at the extremes. However, the behavior is still rather nonlinear in character. Utilizing the same functional form as the charging model, the correlation agrees fairly well with the data as shown in Figure 9.

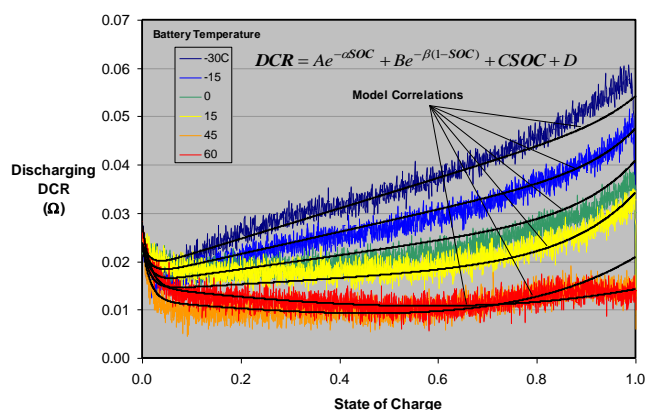


**Figure 9:** Discharging DCR Data and Model Correlation as a function of Battery SOC and Temperature

Coefficient data obtained from least squared error minimization for the discharging resistance model are shown in Table 4.

**Table 4:** Discharging Resistance Model Temperature Coefficients

Coefficient	m	b
<i>A</i>	5.698E-03	4.647E-03
<i>B</i>	1.455E-02	2.159E-03
<i>α</i>	3.133E-01	6.282E+01
<i>β</i>	-7.978E+00	1.385E+01
<i>C</i>	-3.714E-02	3.712E-02
<i>D</i>	-6.255E-03	1.935E-02

At the extremes of the temperature range, the model correlation tends to deviate from data. This is a result of a nonlinear coefficient temperature response. Further investigations are underway to characterize this effect in greater detail.

#### ALGORITHM DEVELOPMENT TESTING

The Tank-Automotive Research, Development Engineering Center (TARDEC) has developed and proposed a new variable voltage charging algorithm to improve battery charging. The second phase of testing will execute the same experimental protocols employing the new TARDEC algorithm for variable charge voltage to provide comparative results. The Advanced Battery Tester can generate programmable output and control to facilitate these tests.

Once the comparative testing is completed, the third phase of testing will focus around a more realistic apparatus designed to simulate vehicle operations. This apparatus has been designed and fabricated to simulate vehicle operations

in a controlled laboratory environment. A schematic of the overall vehicle simulation is depicted in Figure 10.

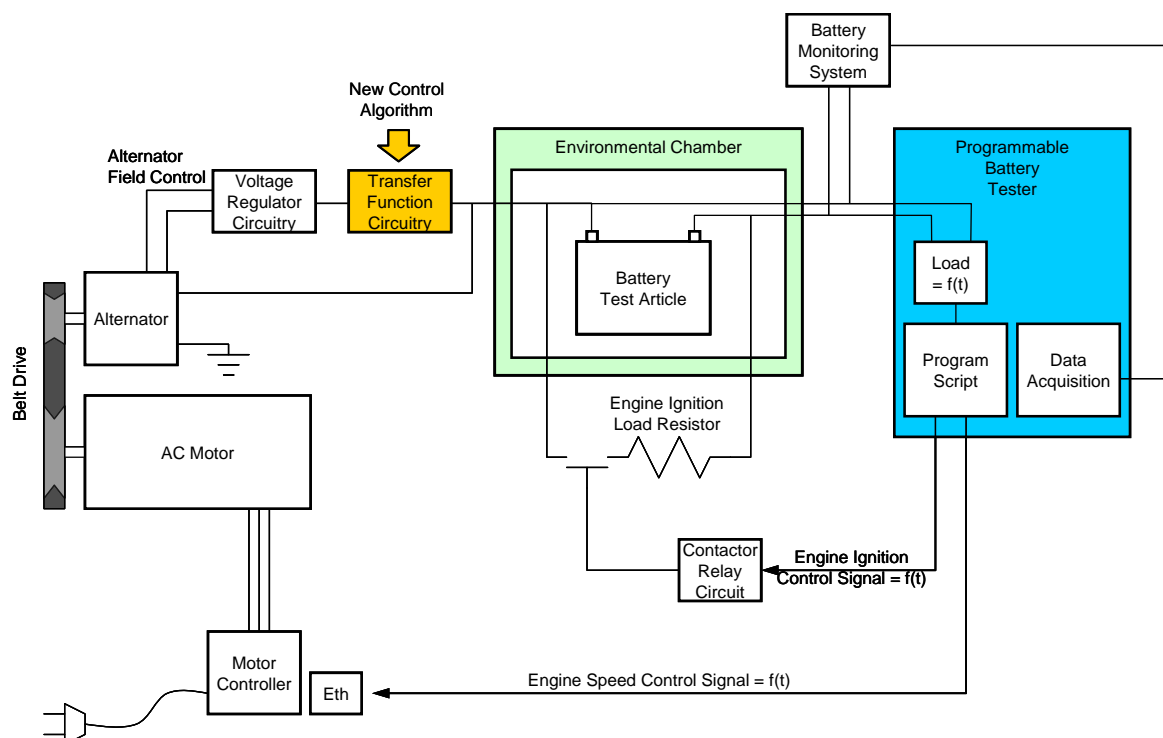


**Figure 10:** Schematic of Vehicle Simulation Apparatus

This third phase of testing will employ a more dynamic response through simulation of a vehicle charging system. A military alternator is driven with a variable speed electric motor to simulate a vehicle engine drive system. Through control with the Advanced Battery Tester, the apparatus setup allows for dynamic simulation of vehicle start sequences, driving scenarios, and silent watch operations. The alternator control voltage is adjusted through a programmable transfer function to allow dynamic power output control as a function of battery conditions.

The Battery test article will be maintained in the environmental chamber to allow testing over a range of ambient conditions. The battery can power two independent loads. The first is a relay-controlled load resistor to simulate engine starter power consumption. The second is a programmable load within the Advanced Battery Tester to simulate vehicle auxiliary loads. Battery recharging will be performed by the speed-controlled alternator and the transfer function circuitry to provide alternator voltage feedback control.

The Advanced Battery Tester provides programmable control of the electric motor and therefore alternator speed, ignition circuit relay operations and the vehicle load current demands. It also provides data collection and storage.

One key aspect this experiment will look to demonstrate is improved operations for vehicle silent watch operations. The proposed silent watch profile is depicted in Figure 11. The profile begins with an extended silent watch profile with time varying current demand. Following a short rest, an engine starting sequence will be executed followed by a constant voltage recharge. Tests will be repeated over a range of ambient temperatures.

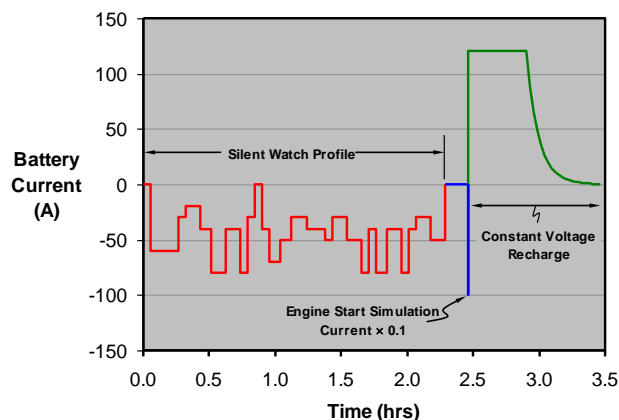


**Figure 11:** Silent Watch Testing Profile



This first stage of the silent watch profile testing phase will then be repeated to provide comparison to the voltage variant recharging algorithms. Although the silent watch profile current demand has been developed for a pair of batteries, it is expected that the results derived from this testing can be readily extended to infer performance for larger battery arrays.

The vehicle simulation apparatus can be used for a variety of testing scenarios. Through the motor control, realistic driving profiles can be simulated to account for changes in engine speed. As a supplement to providing optimized battery recharging, the apparatus can also be used to capture dynamic alternator efficiency performance.

### **Battery Monitoring System Testing**

As a complement to the dynamic charging algorithm testing, the experiment will look to provide verification testing on a commercially-available lead acid battery monitoring system (BMS).

During silent watch operations, it is imperative to maintain knowledge about the battery SOC. This knowledge is important to ensure adequate reserves are maintained for vehicle ignition. An accurate BMS can provide feedback to the vehicle operator to ensure functionality is maintained.

BMS data will be compared to data collected by the experiment apparatus to establish accuracy, estimate calibration time frames, and provide a component assessment. Further, the BMS data will be compared to the empirically established battery model performance to ensure accuracy is maintained.

### **CONCLUDING REMARKS**

A sequence of performance tests have been developed and are under execution for the improvement of battery charging algorithms with the goal of enhancing battery lifetime, performance and knowledge status. The first stage of testing focused on the battery performance as a function of environmental conditions. Model development is underway to characterize equivalent circuit parameters as a function of battery SOC and temperature.

An apparatus has been designed and fabricated to simulate realistic vehicle operations under a range of operational and environmental conditions. Near term testing using the vehicle simulation apparatus will provide comparisons between charging algorithms and simulation of vehicle operations during silent watch operations.

### **REFERENCES**

[1] C.E.Niehoff & Co., Alternator Specification, N3240 Voltage Regulator, 2012.

- [2] M. Ceraolo, Dynamical Models of Lead-Acid Batteries, IEEE Transactions on Power Systems, vol. 15, pp. 1184-1190, Nov. 2000.
- [3] M. Chen and G.A. Rincon-Mora, Accurate Electrical Battery Model Capable of Predicting Runtime and I-V Performance, IEEE Transactions on Energy Conversion, 21(2): 504-5011, 2006.
- [4] H.L. Chan and S. Suntanto, A New Battery Model for Use with Energy Storage Systems and Electric Vehicles Power Systems, Proceedings of the IEEE Winter Meeting, Vol. 1, Jan, 23-27, 2000, pp. 470-475.
- [5] A. Fasih, Modeling and Fault Diagnosis of Automotive Lead-Acid Batteries, Master's Thesis, Ohio State University, 2006.
- [6] S. Barsali and M. Ceraolo, Dynamical Models of Lead-Acid Batteries: Implementation Issues, IEEE Transactions on Energy Conversion, 17(1), 16-23, 2002.
- [7] MIL-PRF-32143A(AT), Performance Specification – Batteries, Storage: Automotive Valve Regulated Lead Acid (VRLA), September 2006.